

<https://doi.org/10.1038/s41531-025-00921-4>

Exploring glymphatic system alterations in iRBD and Parkinson's disease using automated DTI-ALPS analysis

Check for updates

S. Marecek¹ ✉, V. Rottova¹, J. Nepozitek¹, T. Krajca², R. Krupicka², J. Keller³, D. Zogala⁴, J. Trnka⁴, K. Sonka¹, E. Ruzicka¹ & P. Dusek¹

Diffusion tensor image analysis along the perivascular space (DTI-ALPS) is a potential non-invasive marker of glymphatic function that typically relies on manual region of interest (ROI) placement. This study compared ALPS indices in treatment-naïve, de novo diagnosed patients with Parkinson's disease (PD), patients with isolated REM behavior disorder (iRBD), and healthy controls using both manual and automatic approaches to the ROI selection used in ALPS-index calculation. ALPS indices were analyzed bilaterally and correlated with clinical severity (MDS-UPDRS) and nigrostriatal denervation (DAT-SPECT). ANCOVA revealed significant inter-group differences using both manual ($p = 0.018$) and automatic ($p = 0.002$) ROI selection methods. The automatic ROI selection approach showed significantly lower ALPS indices in PD compared to controls ($p = 0.001$) and iRBD ($p = 0.009$). ALPS indices correlated with symptom severity and nigrostriatal denervation. These findings underscore the reliability of the automatic ROI placement approach for ALPS index calculation and may indicate early glymphatic alterations in Parkinson's disease.

The glymphatic system is a whole-brain perivascular network that utilizes periarterial cerebrospinal fluid (CSF) influx, with its subsequent diffusion into the brain parenchyma and perivenous efflux to drive interstitial solute clearance^{1,2}. Dysfunction of the glymphatic system is increasingly recognized as a contributing factor in several neurological disorders, including Parkinson's disease (PD), normal pressure hydrocephalus, Alzheimer's disease, and others^{3–6}. The pathophysiological mechanisms of glymphatic dysfunction in PD are not well known. However, one study in mice has shown α -synuclein injection into basal ganglia caused delayed dural lymphatic vessel drainage, and vice versa, the ligation of draining lymphatic vessels caused increased α -synuclein accumulation and exacerbated motor and memory deficits⁷. In PD, glymphatic dysfunction has been observed even in the earliest stages of neurodegeneration, including its prodromal stages, represented by isolated rapid-eye-movement behavior disorder (iRBD)^{8,9}.

RBD is a disorder characterized by dream enactment and loss of muscle atonia during REM sleep. It can be caused by narcolepsy, antidepressant intake, brainstem lesions; when a precise cause has not been identified, it is termed 'isolated' RBD. This isolated RBD (iRBD) is predominantly caused by early-stage synucleinopathies, with studies

showing an approximate 70% conversion rate over 12 years to either PD, dementia with Lewy bodies, or multiple system atrophy^{10–12}. This makes iRBD a valuable target for studying PD's pathophysiology, course, and possible therapy^{13,14}.

There are several potential ways to measure the function of the glymphatic system¹⁵, with diffusion tensor imaging along perivascular spaces (DTI-ALPS)—first described in 2017 by Taoka et al.¹⁶—being one of them. This method employs widely available MRI sequences and relies on the placement of regions of interest (ROI) next to the top of the lateral ventricles, into the areas of projection and association fibers. In these areas, the glymphatic flow traverses the perivascular spaces, perpendicular to the lateral ventricles and both the projection and association fibers. Diffusion tensor imaging can be used to estimate the movement of water along these perivascular spaces, theoretically reflecting the functionality of the glymphatic system⁶. However, one of the main critiques of the DTI-ALPS method is the lack of rigorous pathophysiological studies demonstrating its relationship to glymphatic function⁶. Nevertheless, one study reported a good correlation between glymphatic system functionality, as measured by intrathecal gadolinium injection, and the DTI-ALPS method¹⁷.

¹Department of Neurology and Center of Clinical Neuroscience, First Faculty of Medicine, Charles University and General University Hospital in Prague, Prague, Czech Republic. ²Czech Technical University in Prague, Faculty of Biomedical Engineering, Kladno, Czech Republic. ³Department of Radiodiagnostics, Na Homolce Hospital, Prague, Czech Republic. ⁴Institute of Nuclear Medicine, First Faculty of Medicine, Charles University and General University Hospital in Prague, Prague, Czech Republic. ✉e-mail: stanislav.marecek@vfn.cz



To the best of our knowledge, only two studies simultaneously compared patients with PD, iRBD, and healthy controls^{9,18}. In one of these studies, iRBD patients were diagnosed based on history rather than polysomnography, classifying them as “possible” iRBD cases¹⁸. In the other study, each group was limited to only 20 participants⁹. In our study, we aim to compare the glymphatic function—as measured by DTI-ALPS—in newly diagnosed treatment naïve patients with PD, patients with video-polysomnography-confirmed iRBD and healthy controls. Additionally, we explore the relationship between the ALPS-index, clinical scores and nigrostriatal dopaminergic denervation measured by dopamine transporter single-photon emission computed tomography (DAT-SPECT). Furthermore, most of the studies using the DTI-ALPS method employ a manual selection of regions of interest (ROIs)⁶. This introduces the possibility of human error or bias. We aimed to employ an automatic ROI selection algorithm that would forego the need for selection of these ROIs by clinicians.

Results

Subject characteristics

Our study cohort initially comprised 91 patients with PD, 68 patients with iRBD, and 50 control subjects. Of these, 12 subjects were excluded due to preprocessing failures—specifically, failures during the *topup* step and the subsequent transformation to normalized space. One patient was excluded owing to a structural abnormality, and an additional 12 subjects were removed because an eccentric head position precluded the identification of manual regions of interest (ROIs). In total, 25 subjects were excluded, yielding a final sample of 79 PD patients, 57 iRBD patients, and 48 controls (Table 1).

The iRBD group was significantly older than both the PD and control groups, comprised a higher proportion of males than the PD group, and exhibited lower MoCA scores compared to the control group. Notably, the MoCA scores remained significantly lower in the iRBD group relative to controls even after controlling for age and sex ($p = 0.009$).

The PD group demonstrated significantly higher MDS-UPDRS parts II and III scores than both the iRBD and control groups, and significantly higher MDS-UPDRS part I scores than the control group. Additionally, the

iRBD group showed significantly higher MDS-UPDRS parts I and II scores compared to the control group and higher MDS-UPDRS part I scores than the PD group.

Reliability analysis of manual and automatic ROI selection approaches

To evaluate the reliability of the ALPS indices derived from our ROI selection approaches—manual and automatic—we compared the three ALPS indices (average, left-hemisphere, and right-hemisphere) obtained by each approach.

ALPS indices calculated via manual ROI selection were significantly higher than those obtained using the automatic approach (manual: mean = 1.30, SD = 0.18; automatic: mean = 1.23, SD = 0.16; $t(183) = 9.334$, $p < 0.001$, Cohen’s $d = 0.41$). This significant difference was also observed for both the left-hemisphere ($p = 0.001$) and right-hemisphere ($p < 0.001$) ALPS indices.

A strong association was found between the ALPS indices obtained from the two ROI selection approaches: for the average ALPS index, $r(182) = 0.83$ ($p < 0.001$); for the left-hemisphere ALPS-index, $r(182) = 0.80$ ($p < 0.001$); and for the right-hemisphere ALPS-index, $r(182) = 0.75$ ($p < 0.001$). Scatter plots illustrating these relationships are presented in Fig. 1.

Bland–Altman plots were generated using the numeric differences between the ALPS indices from the manual and automatic methods (Fig. 1). In these plots, fewer than 10% of subjects fell outside the 95% limits of agreement. As the values of all three ALPS indices increased, a significant ($p < 0.05$) rise in the absolute differences between the automatic and manual ROI selection approaches was observed. When differences were expressed as percentages, this relationship was maintained for the left- and right-hemisphere ALPS indices, though not for the average ALPS-index.

Inter-group differences in ALPS indices

When comparing side-averaged ALPS indices, we found an inter-group difference using both the manual [$F(2,180) = 4.081$, $p = 0.018$] and the automatic [$F(2,180) = 6.448$, $p = 0.002$] ROI selection approaches. In the

Table 1 | Comparison of demographic and clinical characteristics, and of ALPS indices in PD, iRBD, and controls

Characteristics	Controls (n = 48)	iRBD (n = 57)	PD (n = 79)	Inter-group p value	Partial η^2	Between groups p values		
						PD vs. HC	PD vs. iRBD	iRBD vs. HC
Male sex (%)	34 (71)	49 (86)	48 (61)	0.006	–	n.s.	0.001	n.s.
Age (years)	61.5 ± 9.9	66.5 ± 7.2	59.5 ± 12.0	<0.001	–	n.s.	<0.001	0.013
MoCA	25.6 ± 2.4	23.7 ± 2.8	24.7 ± 3.1	0.031*	–	n.s.	n.s.	0.009
MDS-UPDRS I	3.0 ± 2.7	7.5 ± 5.3	5.8 ± 4.3	<0.001*	–	0.001	0.049	<0.001
MDS-UPDRS II	0.7 ± 1.5	2.6 ± 3.9	7.5 ± 4.9	<0.001*	–	<0.001	<0.001	0.016
MDS-UPDRS III	3.4 ± 4.0	6.1 ± 5.4	30.3 ± 13.1	<0.001*	–	<0.001	<0.001	n.s.
Disease duration**	–	8.2 ± 8.5	2.0 ± 1.8	–	–	–	–	–
<i>ALPS indices calculated using manually selected ROIs</i>								
Average	1.35 ± 0.17	1.31 ± 0.16	1.28 ± 0.19	0.018*	0.043	0.008	n.s.	n.s.
Left hemisphere	1.31 ± 0.16	1.27 ± 0.17	1.26 ± 0.20	n.s.*	–	–	–	–
Right hemisphere	1.40 ± 0.23	1.35 ± 0.18	1.31 ± 0.20	0.009*	0.051	0.004	0.028	n.s.
<i>ALPS indices calculated using automatically selected ROIs</i>								
Average	1.28 ± 0.11	1.24 ± 0.14	1.21 ± 0.18	0.002*	0.067	0.001	0.009	n.s.
Left hemisphere	1.29 ± 0.11	1.25 ± 0.14	1.22 ± 0.19	0.003*	0.063	0.001	0.018	n.s.
Right hemisphere	1.27 ± 0.13	1.24 ± 0.14	1.20 ± 0.18	0.003*	0.061	0.003	0.009	n.s.

Where applicable, the data are presented as mean ± standard deviation, with ALPS indices adjusted for age.

MoCA Montreal Cognitive Assessment, MDS-UPDRS Movement Disorder Society-Sponsored Revision of the Unified Parkinson’s Disease Rating Scale, HC healthy controls, n.s. not significant, bold for $p < 0.05$.

*Adjusted for age and sex.

**Disease duration is defined as the subjective duration of dream enactment behavior in iRBD and time since the occurrence of the first motor symptom in PD.

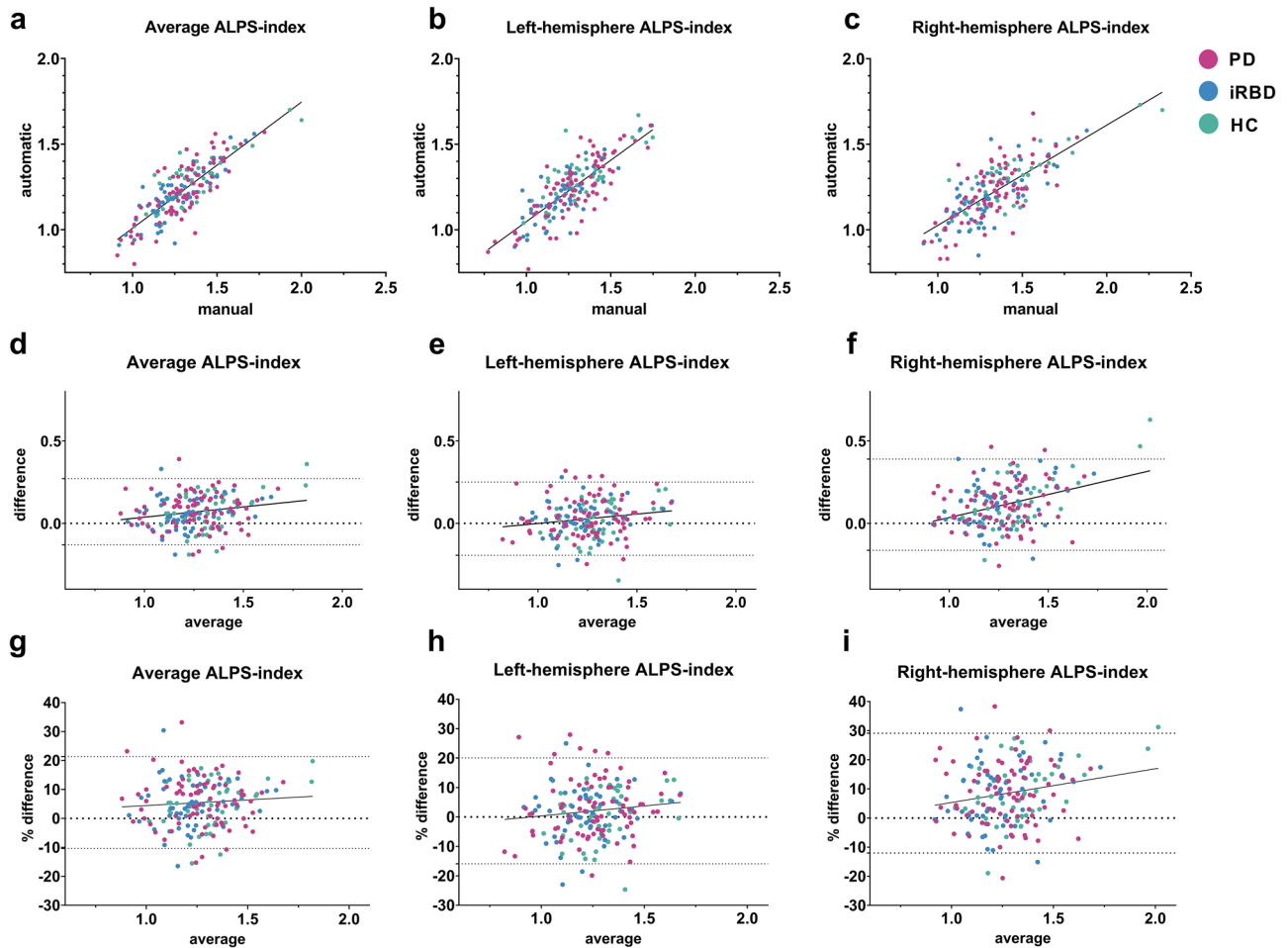


Fig. 1 | Analysis of differences in manual and automatic approaches to ROI selection used in ALPS-index calculation. Scatter plots representing the relation of manual and automatic ROI selection approaches (a–c). Bland–Altman plots using

the numeric difference values (d–f) and % difference values (g–i) between the manual and automatic approaches.

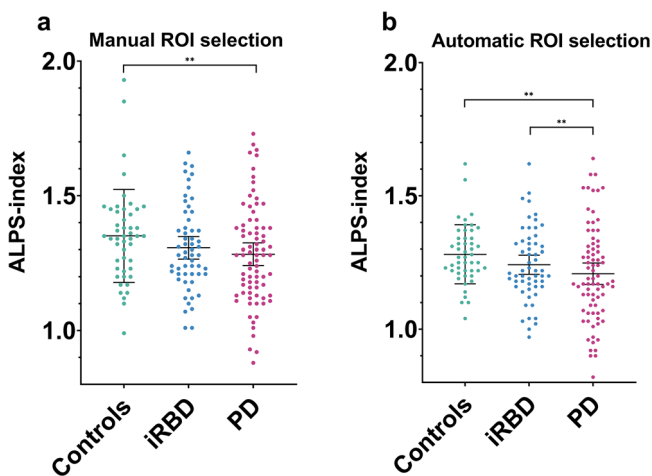


Fig. 2 | Differences in ALPS indices between PD, iRBD, and HCs. Scatter plots displaying differences in ALPS indices calculated using the manual (a) and automatic (b) ROI selection methods in PD, iRBD, and HCs. Volumes are adjusted for age, and the lines and whiskers represent the mean and standard deviations, respectively. **for $p < 0.01$.

post-hoc analysis, PD subjects had lower ALPS indices using both the manual [$p = 0.008$, $p = 0.051$ (PD vs. controls, PD vs. iRBD)] and automatic [$p = 0.001$, $p = 0.009$ (PD vs. controls, PD vs. iRBD)] ROI selection approaches (Fig. 2, Table 1).

The results in left- and right-sided age-adjusted ALPS indices were comparable to the average values, except for the left-sided ALPS indices calculated via the manual ROI selection approach, where no inter-group difference was found (Table 1).

As the iRBD group was significantly older than the PD group and had significantly more male participants, we performed a sensitivity analysis in age- and sex-matched subgroups. This yielded 40 participants in each group. Using identical methods, we found an inter-group difference in the automatic approach [$F(2,116) = 5.607$, $p = 0.005$], with the PD group having significantly lower ALPS indices [$p = 0.003$, $p = 0.007$ (PD vs. controls, PD vs. iRBD)]. We did not find any significant inter-group differences using the manual approach ($p = 0.067$).

Effects of nigrostriatal denervation

We found a positive correlation between ALPS indices and mean putaminal SBR Z-scores using both the manual [$p = 0.029$, $r(129) = 0.191$] and automatic [$p < 0.001$, $r(129) = 0.310$] approaches in the PD-iRBD pooled group (Fig. 3). When analyzing the PD group separately, the correlation remained significant for both the manual [$p = 0.027$, $r(76) = 0.250$] and automatic [$p = 0.011$, $r(76) = 0.286$] approaches.

Similar results were observed for caudate SBR Z-scores. In the PD-iRBD pooled group, ALPS indices calculated using ROIs selected by the automatic method showed a significant correlation [$p < 0.001$, $r(129) = 0.306$]; however, the manual selection method did not yield a significant correlation ($p = 0.051$) (Fig. 3). When analyzing the PD

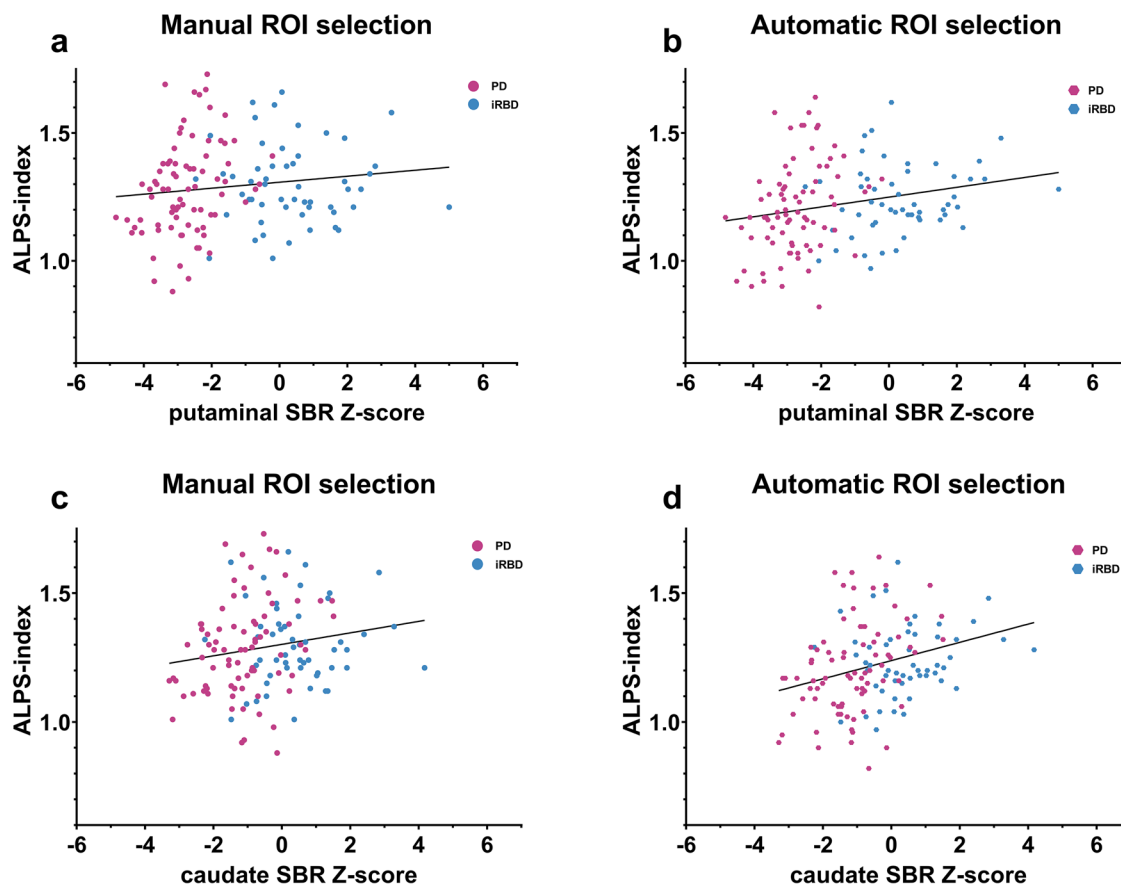


Fig. 3 | Average putaminal and caudate SBR Z-scores in relation to ALPS indices. Scatter plots illustrating the relationship between average putaminal and caudate SBR Z-scores and ALPS indices calculated using both the manual and automatic ROI selection approaches. Panel a shows the manual approach for putaminal SBR

Z-scores, panel b the automatic approach for putaminal SBR Z-scores, panel c the manual approach for caudate SBR Z-scores, and panel d the automatic approach for caudate SBR Z-scores. Volumes adjusted to age. PD and iRBD subjects are pooled.

Table 2 | Associations between ALPS indices calculated using manual and automatic ROI selection approaches and symptom severity in Parkinson’s disease

	MDS-UPDRS I	MDS-UPDRS II	MDS-UPDRS III	Tremor	Rigidity	Bradykinesia	Axial
Manual	0.005(−0.32)	<0.001(−0.45)	0.002(−0.35)	0.665(−0.05)	0.135(−0.172)	<0.001(−0.41)	0.003(−0.34)
Automatic	0.055(−0.22)	0.001(−0.36)	0.028(−0.25)	0.626(0.06)	0.220(−0.14)	0.006(−0.31)	0.001(−0.37)

Using two-tailed partial correlation on age-adjusted ALPS indices, controlling for age and sex Values presented as *p*-value (partial correlation coefficient). Bold for *p* < 0.05.

group separately, the correlation remained significant only for the automatic approach [*p* = 0.039, *r*(76) = 0.234] but not for the manual approach (*p* = 0.211).

We further compared ALPS indices between the most affected and least affected hemispheres with respect to putaminal and caudate SBR Z-scores on DAT-SPECT. No significant differences were found between the most and least affected hemispheres in the pooled group or when analyzing the PD and iRBD groups separately.

Associations with clinical features

Several negative correlations were found between ALPS indices and MDS-UPDRS scores in patients with PD (Table 2). Specifically, the manual ROI selection approach was correlated with the MDS-UPDRS I score, while both manual and automated ROI selection approaches were correlated with the MDS-UPDRS II and III scores. Additionally, ALPS indices were correlated with the bradykinesia and axial subscores of the MDS-UPDRS III in PD.

In contrast, no significant correlations were observed between age-adjusted ALPS indices and MoCA scores in any of the groups.

Discussion

Our results show lower ALPS indices—indicating decreased diffusion in the direction of glymphatic flow—in patients with PD compared to patients with iRBD and healthy controls. Moreover, this decrease correlates with nigrostriatal denervation, as measured by DAT-SPECT, and clinical severity, as measured by MDS-UPDRS clinical scales.

The DTI-ALPS method, first described by Taoka et al. in 2017¹⁶, is a relatively new approach for measuring glymphatic system dysfunction. As such, the method still lacks rigorous pathological verification^{6,19} to prove that ALPS-index represents the actual magnitude of glymphatic flow. However, at least one study did show a correlation with glymphatic system function as measured by intrathecal application of gadolinium¹⁷.

Another critique of the DTI-ALPS method is the possibility of human error during the ROI selection process. We addressed this issue by incorporating an automatic ROI selection approach, which, based on our findings, demonstrated performance comparable to or superior to that of the manual method. Our approach was similar to other studies that employed an atlas-based method for ROI selection—one study used a similar JHU atlas²⁰, while others used the ICBM DTI-81 atlas^{4,21}.

When comparing the manual and automatic approaches for ROI selection, we found that ALPS indices calculated using the manual approach were significantly higher than those obtained via automatic ROI selection. Bland-Altman plots further revealed that the difference between the methods increased with higher ALPS indices, although only a small number of subjects fell outside the 95% limits of agreement. Nevertheless, the correlation between the methods was excellent.

In our study, all ALPS indices (average, left, right, calculated using both manual and automatic ROI selection approaches) showed similar results, except the left-hemisphere ALPS indices calculated using the manual approach, which did not show significant between-group differences. This finding is unexpected, as the placement of left-sided association ROIs is generally easier since the superior longitudinal fasciculus of right-handed subjects is better discernible on the usually dominant left side (as most of the population is right-handed)⁶. This could be due to human error during ROI selection, which highlights the need for automated ROI selection. Future studies should verify the performance of different atlases in automatic DTI-ALPS calculation.

We found two previous studies comparing ALPS indices in PD, iRBD, and healthy control subjects. Both found significant differences in ALPS indices between iRBD and control subjects. One study included “probable” iRBD (cases not confirmed by polysomnography) and found significant differences between all three groups¹⁸. The other study included iRBD subjects confirmed by polysomnography and found significant differences between iRBD and HC, but not between iRBD and PD subjects; however, it included only 20 patients in each group⁹. Some previous studies compared ALPS indices in iRBD and control subjects only and found significantly reduced ALPS indices in iRBD subjects⁸. In our study, we did not confirm this finding. This could be due to several reasons, including inter-rater variability in the selection of manual ROIs used in these studies, differences in patient populations, and a relatively low number of iRBD patients, which may have led to limited statistical power. Our iRBD subjects were recruited “on-demand” by a media campaign. This difference—in that patients were approached rather than spontaneously seeking medical help for their iRBD symptoms—could, in our case, select for a different, perhaps earlier-stage, patient population than in previous studies. This is supported by a study by Joza et al.²², which found that self-referral through outreach initiatives was associated with earlier clinical presentation and subsequent slower progression.

We found two studies comparing ALPS indices to DAT-SPECT. One study involved drug-naïve PD patients, while the other focused on individuals with iRBD, neither finding a correlation between ALPS indices and DAT-SPECT^{9,23}. Another study found a correlation between nigral dopaminergic denervation and ALPS indices using a hybrid 18F-fluorodopa PET-MRI²⁴. Even when employing a simpler approach to nigrostriatal denervation imaging, our results indicate that ALPS indices are significantly correlated with the degree of nigrostriatal denervation in PD patients—an association not observed in iRBD patients.

The absence of significant differences in ALPS indices between iRBD patients and healthy controls, together with the observed correlations between ALPS indices, motor impairment (as measured by UPDRS II and III scores), and nigrostriatal denervation in PD, suggests that glymphatic dysfunction may be a dynamic process that worsens with disease progression. However, as the DTI-ALPS method lacks pathological validation, further verification is needed—either of the DTI-ALPS method itself or by using other methods of measuring glymphatic dysfunction. Future studies will also be needed to assess the extent to which glymphatic system dysfunction is accelerated by synucleinopathy, compounding the “physiological” age-related decline in glymphatic flow.

An interesting finding is the correlation of ALPS indices with MDS-UPDRS scores and bradykinesia and axial MDS-UPDRS III subscores. The correlation with MDS-UPDRS scores has been described before^{23,25}. In a

previous study, the results differed, with ALPS indices correlating with only the rigidity subscores²⁶.

Our study did not find a correlation between ALPS indices and MoCA. There are inconsistent results regarding the correlation between cognitive dysfunction and ALPS indices. Some studies did not find a correlation between ALPS indices and MoCA^{18,26}, whereas others described a relationship between cognitive dysfunction and ALPS indices⁵. However, our subjects were in a very early stage of the disease. As overt cognitive deficit is not a feature of iRBD or generally of early-stage PD, it is possible that the association would appear at later stages, when a larger spread of MoCA scores might be observed due to the onset of dementia in a subset of patients.

The finding of significantly higher rates of non-motor signs (as measured by UPDRS Part I) in iRBD patients compared to both PD and HC subjects was previously described in a paper by Barber et al.²⁷, in which an analysis of a large cohort of iRBD and de novo PD patients showed similar results. In that study, the iRBD patients exhibited higher scores for depression, apathy, and anxiety compared to those with established PD. A possible explanation given was that PD patients who progress from iRBD tend to exhibit the akinetic-rigid/postural instability-gait difficulty subtype²⁸, which is associated with a more severe non-motor phenotype²⁹. This is also in line with the observation that iRBD relates to the “diffuse malignant” or “body first” subtype of PD as well as DLB, which is characterized by higher rates of non-motor signs and mild cognitive impairment^{30,31}. Indeed, unlike the PD group, iRBD patients in this study had significantly lower MoCA scores than healthy controls.

The higher age observed in the iRBD group may be explained by our unselected PD cohort, which includes a proportion of early-onset patients. Multicenter studies indicate that the age of onset for iRBD is generally later than that for unselected PD; for instance, approximately 8% of iRBD patients are younger than 55 years¹², compared to about 27% of PD patients being younger than 56 years³². Moreover, the mean ages reported in these multicenter studies—66.3 years for iRBD and 61.7 years for PD—are roughly in line with the demographic patterns observed in our cohorts.

We also did not find a side difference between the more affected side and the less affected side by nigrostriatal denervation. This could be explained by the glymphatic dysfunction being a global process affected by overall neurodegeneration rather than by “local” side differences in nigrostriatal denervation.

Fluid flow through the glymphatic system is inextricably linked with sleep³³. In the case of the DTI-ALPS method, one study found a connection between sleep disruption—as measured by the Pittsburgh Sleep Quality Index—and decreased ALPS indices³⁴. Another study found that ALPS indices were negatively correlated with blood levels of neurofilament light chain in patients with traumatic brain injury³⁵. In the context of neurodegeneration, a study by Xie et al.³⁶ described a 95% decrease in tracer influx in awake mice compared to sleeping mice, accompanied by a two-fold increase in A β clearance in sleeping mice. This implies a connection between sleep, glymphatic system function, and proteinopathies^{33,37}. However, although sleep disturbances are common in PD³⁸ and patients with PD show impaired meningeal lymphatic function⁷, the precise pathophysiological connections remain to be explored.

In conclusion, our results show a decrease in ALPS indices in PD compared to iRBD and HCs, which could be a sign of glymphatic dysfunction in PD. The ALPS indices in PD correlated with clinical severity as measured by MDS-UPDRS scores and nigrostriatal denervation as measured by DAT-SPECT. This could suggest that glymphatic dysfunction is a dynamic process that worsens with disease progression. The ALPS indices of iRBD patients were numerically intermediate between those of the PD and HC groups, with significant differences observed only between iRBD and PD patients. Moreover, we have shown that an automatic approach to ROI selection is comparable, and in some cases even superior, to the manual approach.

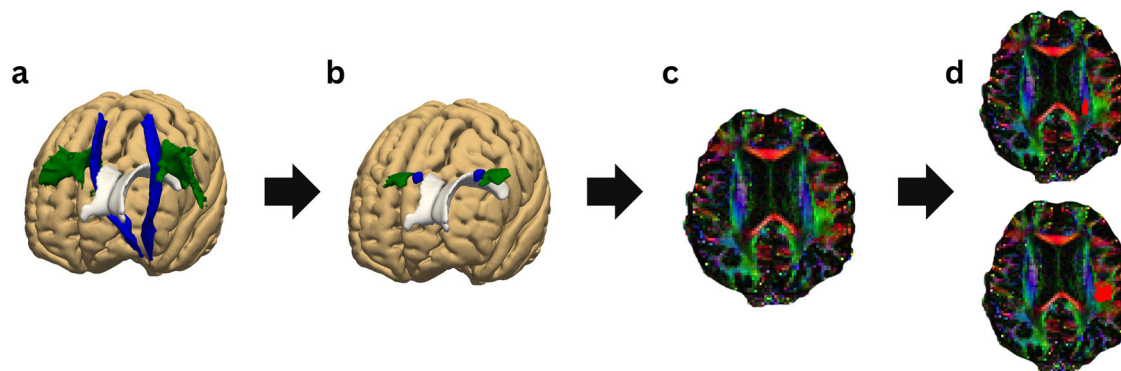


Fig. 4 | Automatic ALPS ROI selection. We used the “JHU ICBM tracts maxprob thr25 1 mm” atlas labels of superior longitudinal fasciculus and corticospinal tract, for the association and projection areas, respectively (a). We restricted these labels to the area on the top of the lateral ventricles and excluded parts close to the cortex (b).

We then calculated a warp from the MNI152 space to each subject’s diffusion space (c) and transformed the masks (d). The images presented in steps c and d display fractional anisotropy-modulated diffusivity in the *x* (red), *y* (green), and *z* (blue) directions.

Methods

Participants

Our subject population consisted of de novo diagnosed treatment-naïve patients with PD, iRBD patients, and healthy controls recruited at the Department of Neurology, First Faculty of Medicine, Charles University and General University Hospital in Prague from 2015 to 2021. The PD patients were part of the BIO-PD cohort described previously³⁹ and were diagnosed according to the Movement Disorders Society (MDS) clinical diagnostic criteria⁴⁰. The iRBD patients were diagnosed in accordance with the International Classification of Sleep Disorders, third edition (ICSD-3) using video-polysomnography⁴¹. Patients with RBD secondary to focal brainstem lesions, narcolepsy, medication usage, and clinically manifest dementia or parkinsonism, were excluded. The control subjects were recruited from the general community via advertisements. Eligibility criteria included the absence of active oncologic illness, significant neurological disorders, and abuse of psychoactive substances. RBD was excluded in all control subjects by history and video-polysomnography. All study participants were examined according to a complex protocol including neurological examination, structured interview, Montreal Cognitive Assessment (MoCA)⁴², and MDS-sponsored Revision of the Unified Parkinson’s Disease Rating Scale (MDS-UPDRS)⁴³. The study was approved by the Ethics Committee of the General University Hospital in Prague (IORG0002175, IRB00002705, FWA00029052). Participants signed informed consent before entering the study, in accordance with the Declaration of Helsinki.

Imaging acquisition protocol

MRI examination was performed on a 3 T scanner (Siemens Skyra 3 T, Siemens Healthcare, Erlangen, Germany) with a 32-channel head coil. The protocol included diffusion tensor MRI with repetition time (TR) = 10.5 s; echo time (TE) = 93 ms; total 72 slices with isotropic voxel resolution of 2 mm; 30 noncolinear directions with *b*-value of 1000 s/m² and one *b* = 0 s/m² image in the anterior–posterior and posterior–anterior phase encoding directions; and an axial 3D T1-weighted Magnetization Prepared Rapid Gradient Echo (MPRAGE, TR 2200 ms; TE 2.4 ms; inversion time (TI) 900 ms; flip angle (FA) 8°; field of view (FOV) 230 × 197 × 176 mm; isotropic voxel resolution 1 mm).

In all PD patients and all but four iRBD patients, DAT-SPECT was performed using the [123I]-2-*b*-carbomethoxy-3-*b*-(4-iodophenyl)-*N*-(3-fluoropropyl) nortropane ([123I]FP-CIT, DaTscan®, GE Healthcare, Little Chalfont, Buckinghamshire, UK) tracer according to European Association of Nuclear Medicine (EANM) procedure guidelines⁴⁴; the detailed protocol is described elsewhere⁴⁵. Automated semi-quantitative analysis was performed using the DaTQUANT v. 2.0 software (GE Healthcare, USA), and the *Z*-scores of specific binding ratios (SBR) in both putamina and caudate

relative to background binding were calculated. DAT-SPECT was performed within one month of MRI. All PD patients were scanned before the introduction of dopaminergic therapy.

Calculating the DTI-ALPS index

For general image preprocessing, we employed FSL^{46,47} and MRtrix3^{48,49}. An automatic processing pipeline was developed using Snakemake^{50,51}, with the most computationally intensive tasks executed on the CESNET MetaCentrum distributed computing infrastructure. All analyses were performed in each subject’s native diffusion space. The DWI data were denoised, corrected for Gibbs ringing artifacts, and adjusted for distortions, eddy currents, and head movement. Subsequently, FSL’s DTIFIT tool was used to generate the *Dxx*, *Dyy*, and *Dzz* diffusivity images.

The DTI-ALPS method is predicated on the placement of regions of interest (ROIs) within the white matter areas of the association and projection fibers adjacent to the apex of the lateral ventricles. In these regions, the perivascular spaces—along which glymphatic flow is oriented—run along the *x*-axis, while association fibers extend along the *y*-axis and projection fibers along the *z*-axis. The ALPS-index is calculated as the ratio of the mean diffusivity along the *x*-axis (which includes the glymphatic flow) to the mean diffusivity along the axes lacking both glymphatic flow and white matter fibers (specifically, the *y*-axis in the projection area and the *z*-axis in the association area), as expressed in Eq. (1):

$$\text{ALPS - index} = \frac{\text{mean}(D_{xx} \text{ projection}, D_{xx} \text{ association})}{\text{mean}(D_{yy} \text{ projection}, D_{zz} \text{ association})} \quad (1)$$

Two methods of ROI selection were employed: manual and automatic. In the manual approach, a blinded rater (V.R.) placed cubic ROIs measuring 6 × 6 × 6 mm within the projection and association white matter regions of both hemispheres. For the automatic approach (Fig. 4), the labels from the “JHU ICBM tracts maxprob thr25 1 mm” atlas corresponding to the superior longitudinal fasciculus (SLF) and corticospinal tract (CST) was used for the association and projection regions, respectively^{52–54}. These labels were restricted to the region at the apex of the lateral ventricles, with portions adjacent to the cortex excluded to prevent potential intrusion during the transformation to each subject’s diffusion space. A single transformation from MNI-152 space to each subject’s diffusion space was generated using FSL via a three-step process: (1) FLIRT’s linear transformation registered each subject’s *b* = 0 diffusion image to their structural T1 image; (2) FLIRT and FNIRT’s non-linear transformations registered the T1 images to the MNI-152 template; and (3) CONVERTWARP produced a unified transformation from the MNI-152 template to each subject’s diffusion space. Finally, the restricted SLF and CST ROIs were transformed into each subject’s diffusion space and binarized, yielding the association and projection ROI masks used in the ALPS-index calculation.

Statistics

Statistical analyses were performed using IBM SPSS for Windows (Version 26). The chi-square test was employed to compare the sex distribution between groups, and a one-way analysis of variance (ANOVA) was applied to assess inter-group differences in age. A one-way analysis of covariance (ANCOVA), with age and sex as covariates, was used to evaluate differences in MDS-UPDRS and MoCA scores. Given the known association between the ALPS-index and age⁵⁵, ALPS indices were adjusted for age using the regression coefficient (β) and the mean age from control subjects as described in Eq. (2)⁵⁶:

$$\text{ALPS} - \text{index}_{\text{adjusted } i} = \text{ALPS} - \text{index}_{\text{raw } i} - \beta (\text{Age}_{\text{raw } i} - \text{Age}_{\text{mean}}) \quad (2)$$

Subsequently, a one-way ANCOVA with sex as a covariate was used to assess inter-group differences in the age-adjusted ALPS indices. All post-hoc multiple comparisons were conducted using the least significant difference (LSD) method, and effect sizes were expressed as partial eta squared (partial η^2).

Partial correlation analyses—with sex as a covariate—were conducted to examine the relationship between age-adjusted ALPS indices and the average putaminal and caudate SBR *Z*-scores from both hemispheres. Additionally, age and sex were included as covariates when investigating correlations with MoCA and MDS-UPDRS scores. This method was also applied to evaluate the correlations between ALPS indices and the following MDS-UPDRS III subscores: tremor (sum of items 15–18), bradykinesia (sum of items 2, 4–9, and 14), rigidity (item 3), and axial (sum of items 1 and 9–13) subscores⁵⁷.

To assess potential side differences in ALPS indices relative to the degree of nigrostriatal denervation, the paired Student's *t*-test was used to compare the side with the higher putaminal SBR *Z*-score against the side with the lower putaminal SBR *Z*-score on DAT-SPECT. The same approach was used for caudate SBR *Z*-scores.

Sensitivity analyses were performed using age- and sex-matched subgroups to mitigate potential bias. Matching was conducted using SPSS's case-control matching utility with a randomized case order for match selection and a tolerance value of 8 years for age and 0 for sex.

Finally, to compare the manual and automatic approaches across all parameters (i.e., average, right-hemisphere, and left-hemisphere ALPS indices), three statistical methods were employed: (1) a paired Student's *t*-test to assess significant differences; (2) bivariate correlation analysis using the Pearson correlation coefficient; and (3) Bland–Altman plots to evaluate agreement based on both numeric and percentage differences between the methods. Additionally, linear regression was performed to investigate the relationship between average ALPS-index values and the differences (both numeric and percentage) between ALPS indices calculated using the manual and automatic ROI selection approaches.

Data availability

The datasets used and analyzed during the current study are available from the corresponding author on request.

Received: 11 December 2024; Accepted: 19 March 2025;

Published online: 15 April 2025

References

1. Iff, J. J. et al. A paravascular pathway facilitates CSF flow through the brain parenchyma and the clearance of interstitial solutes, including amyloid β . *Sci. Transl. Med.* **4**, 147ra111 (2012).
2. Bohr, T. et al. The glymphatic system: current understanding and modeling. *iScience* **25**, 104987 (2022).
3. Kamagata, K et al. Association of MRI indices of glymphatic system with amyloid deposition and cognition in mild cognitive impairment and Alzheimer disease. *Neurology* **99**, E2648–E2660 (2022).
4. Yokota, H et al. Diagnostic performance of glymphatic system evaluation using diffusion tensor imaging in idiopathic normal pressure hydrocephalus and mimickers. *Curr. Gerontol. Geriatr. Res.* **2019**, 5675014 (2019).
5. Shen, T, et al. Diffusion along perivascular spaces as marker for impairment of glymphatic system in Parkinson's disease. *npj Park. Dis.* **8**, 1–10 (2022).
6. Taoka, T. et al. Diffusion tensor image analysis along the perivascular space (DTI-ALPS): revisiting the meaning and significance of the method. *Magn. Reson. Med. Sci.* (2024). <https://doi.org/10.2463/MRMS.REV.2023-0175>.
7. Ding, X. et al. Impaired meningeal lymphatic drainage in patients with idiopathic Parkinson's disease. *Nat. Med.* **27**, 411–418 (2021).
8. Lee, DA, Lee, HJ & Park, KM Glymphatic dysfunction in isolated REM sleep behavior disorder. *Acta Neurol. Scand.* **145**, 464–470 (2022).
9. Bae, Y. J. et al. Altered brain glymphatic flow at diffusion-tensor MRI in rapid eye movement sleep behavior disorder. *Radiology* **307**, e221848 (2023).
10. Mattioli, P et al. Derivation and validation of a phenoconversion-related pattern in idiopathic rapid eye movement behavior disorder. *Mov. Disord.* **38**, 57–67 (2023).
11. Zhang, H et al. Risk factors for phenoconversion in rapid eye movement sleep behavior disorder. *Ann. Neurol.* **91**, 404–416 (2022).
12. Postuma, RB et al. Risk and predictors of dementia and parkinsonism in idiopathic REM sleep behaviour disorder: a multicentre study. *Brain* **142**, 744–759 (2019).
13. Hu, MT REM sleep behavior disorder (RBD). *Neurobiol. Dis.* **143**, 104996 (2020).
14. Iranzo, A. et al. Neurodegenerative disorder risk in idiopathic REM sleep behavior disorder: study in 174 patients. *PLoS ONE* **9**, e0089741 (2014).
15. Naganawa, S & Taoka, T The glymphatic system: a review of the challenges in visualizing its structure and function with MR imaging. *Magn. Reson. Med. Sci.* **21**, 182–194 (2022).
16. Taoka, T et al. Evaluation of glymphatic system activity with the diffusion MR technique: diffusion tensor image analysis along the perivascular space (DTI-ALPS) in Alzheimer's disease cases. *Jpn. J. Radiol.* **35**, 172–178 (2017).
17. Zhang, W. et al. Glymphatic clearance function in patients with cerebral small vessel disease. *Neuroimage* **238**, 118257 (2021).
18. Si, X, et al. Neuroimaging evidence of glymphatic system dysfunction in possible REM sleep behavior disorder and Parkinson's disease. *npj Park. Dis.* **8**, 1–9 (2022).
19. Ringstad, G Glymphatic imaging: a critical look at the DTI-ALPS index. *Neuroradiology* **66**, 157–160 (2024).
20. Jiang, D et al. Regional glymphatic abnormality in behavioral variant frontotemporal dementia. *Ann. Neurol.* **94**, 442–456 (2023).
21. Wood, K. H. et al. Diffusion tensor imaging-along the perivascular-space index is associated with disease progression in Parkinson's disease. *Mov. Disord.* <https://doi.org/10.1002/MDS.29908> (2024).
22. Joza, S et al. Is REM sleep behavior disorder changing? Secular changes versus referral patterns. *Mov. Disord. Clin. Pract.* **10**, 1519–1524 (2023).
23. Bae, YJ et al. Glymphatic function assessment in Parkinson's disease using diffusion tensor image analysis along the perivascular space. *Park. Relat. Disord.* **114**, 105767 (2023).
24. Yao, J et al. Early detection of dopaminergic dysfunction and glymphatic system impairment in Parkinson's disease. *Park. Relat. Disord.* **127**, 107089 (2024).
25. Chen, HL et al. Associations among cognitive functions, plasma DNA, and diffusion tensor image along the perivascular space (DTI-ALPS) in patients with Parkinson's disease. *Oxid. Med. Cell. Longev.* **2021**, 4034509 (2021).

26. Qin, Y et al. Neuroimaging uncovers distinct relationships of glymphatic dysfunction and motor symptoms in Parkinson's disease. *J. Neurol.* **270**, 2649–2658 (2023).
27. Barber, T. R. et al. Prodromal Parkinsonism and neurodegenerative risk stratification in REM sleep behavior disorder. *Sleep* **40**, zsx071 (2017).
28. Iranzo, A, Santamaria, J & Tolosa, E Idiopathic rapid eye movement sleep behaviour disorder: diagnosis, management, and the need for neuroprotective interventions. *Lancet Neurol.* **15**, 405–419 (2016).
29. Ba, F, Obaid, M, Wieler, M, Camicioli, R & Martin, WRW Parkinson disease: the relationship between non-motor symptoms and motor phenotype. *Can. J. Neurol. Sci.* **43**, 261–267 (2016).
30. Horsager, J & Borghammer, P Brain-first vs. body-first Parkinson's disease: an update on recent evidence. *Park. Relat. Disord.* **122**, 106101 (2024).
31. Johansson, M. E., van Lier, N. M., Kessels, R. P. C., Bloem, B. R. & Helmich, R. C. Two-year clinical progression in focal and diffuse subtypes of Parkinson's disease. *NPJ Park. Dis.* **9**, 29 (2023).
32. Simuni, T et al. Longitudinal change of clinical and biological measures in early Parkinson's disease: Parkinson's progression markers initiative cohort. *Mov. Disord.* **33**, 771 (2018).
33. Nedergaard, M. & Goldman, S. A. Glymphatic failure as a final common pathway to dementia. *Science* **370**, 50–56 (2020).
34. Saito, Y, et al. Glymphatic system impairment in sleep disruption: diffusion tensor image analysis along the perivascular space (DTI-ALPS). *Jpn. J. Radiol.* **41**, 1335–1343 (2023).
35. Butler, T. et al. Glymphatic clearance estimated using diffusion tensor imaging along perivascular spaces is reduced after traumatic brain injury and correlates with plasma neurofilament light, a biomarker of injury severity. *Brain Commun.* **5**, fca134 (2023).
36. Xie, L et al. Sleep drives metabolite clearance from the adult brain. *Science (80-)* **342**, 373–377 (2013).
37. Nepozitek, J., Dusek, P. & Sonka, K. Glymphatic system, sleep, and Parkinson's disease: interconnections, research opportunities, and potential for disease modification. *Sleep* **48**, zsa251 (2025).
38. Menza, M, Dobkin, RDF, Marin, H & Bienfait, K Sleep disturbances in Parkinson's disease. *Mov. Disord.* **25**, S117 (2010).
39. Dušek, P et al. Clinical characteristics of newly diagnosed Parkinson's disease patients included in the longitudinal BIO-PD study. *Ces. Slov. Neurol. Neurochir.* **83**, 633–639 (2020).
40. Postuma, RB et al. MDS clinical diagnostic criteria for Parkinson's disease. *Mov. Disord.* **30**, 1591–1601 (2015).
41. American Academy of Sleep Medicine. *International Classification of Sleep Disorders* (American Academy of Sleep Medicine, 2014).
42. Nasreddine, ZS et al. The Montreal Cognitive Assessment, MoCA: a brief screening tool for mild cognitive impairment. *J. Am. Geriatr. Soc.* **53**, 695–699 (2005).
43. Goetz, CG et al. Movement Disorder Society-sponsored revision of the Unified Parkinson's Disease Rating Scale (MDS-UPDRS): scale presentation and clinimetric testing results. *Mov. Disord.* **23**, 2129–2170 (2008).
44. Darcourt, J et al. EANM procedure guidelines for brain neurotransmission SPECT using (123)I-labelled dopamine transporter ligands, version 2. *Eur. J. Nucl. Med. Mol. Imaging* **37**, 443–450 (2010).
45. Dušek, P. et al. Relations of non-motor symptoms and dopamine transporter binding in REM sleep behavior disorder. *Sci. Rep.* **9**, 15463 (2019).
46. Jenkinson, M., Beckmann, C. F., Behrens, T. E. J., Woolrich, M. W. & Smith, S. M. FSL. *Neuroimage* **62**, 782–790 (2012).
47. Woolrich, M. W. et al. Bayesian analysis of neuroimaging data in FSL. *Neuroimage* **45**, S173–S186 (2009).
48. Veraart, J et al. Denoising of diffusion MRI using random matrix theory. *Neuroimage* **142**, 394–406 (2016).
49. Tournier, JD et al. MRtrix3: a fast, flexible and open software framework for medical image processing and visualisation. *Neuroimage* **202**, 116137 (2019).
50. Mölder, F et al. Sustainable data analysis with Snakemake. *F1000Research* **10**, 33 (2021).
51. Krajča, T, Mareček, S, Sojka, P, Dušek, P & Krupička, R Streamlining neuroimaging—snakemake's role in developing a striatal segmentation pipeline. *IFMBE Proc.* **110**, 610–617 (2024).
52. Proctor, MR MRI atlas of human white matter. *Am. J. Neuroradiol.* **27**, 1384 (2006).
53. Wakana, S et al. Reproducibility of quantitative tractography methods applied to cerebral white matter. *Neuroimage* **36**, 630–644 (2007).
54. Hua, K et al. Tract probability maps in stereotaxic spaces: analyses of white matter anatomy and tract-specific quantification. *Neuroimage* **39**, 336 (2008).
55. Hsiao, WC et al. Association of cognition and brain reserve in aging and glymphatic function using diffusion tensor image-along the perivascular space (DTI-ALPS). *Neuroscience* **524**, 11–20 (2023).
56. Voevodskaya, O The effects of intracranial volume adjustment approaches on multiple regional MRI volumes in healthy aging and Alzheimer's disease. *Front. Aging Neurosci.* **6**, 93610 (2014).
57. Li, X, Xing, Y, Martin-Bastida, A, Piccini, P & Auer, DP Patterns of grey matter loss associated with motor subscores in early Parkinson's disease. *NeuroImage Clin.* **17**, 498–504 (2018).

Acknowledgements

The study was supported by: National Institute for Neurological Research (Program EXCELES, ID Project No. LX22NPO5107)—Funded by the European Union—Next Generation EU; General University Hospital in Prague project MH CZ-DRO-VFN64165 and Na Homolce Hospital project CZ-DRO-NHH00023884 and Czech Health Research Council grant NU21-04-00535. Computational resources were provided by the e-INFRA CZ project (ID:90254), supported by the Ministry of Education, Youth and Sports of the Czech Republic. Access to CESNET storage facilities provided by the project „e-INFRA CZ“ under the program „Projects of Large Research, Development, and Innovations Infrastructures“ LM2018140 is greatly appreciated.

Author contributions

S.M. co-designed the study concept, implemented the preprocessing and automatic segmentation algorithm, performed statistical analysis, and wrote the draft of the manuscript. V.R. co-designed the study concept and managed the manual placement of ROIs. J.N. co-designed the study concept and performed the polysomnography analysis. T.K. managed the resource-intensive computing on MetaCentrum and automated the algorithm. R.K. advised on automated algorithm creation and statistical analysis. J.K. contributed to MRI acquisition. D.Z. contributed to DAT-SPECT acquisition and processing. J.T. contributed to DAT-SPECT acquisition and processing. K.S. contributed to the polysomnography acquisition and processing and to the critical edition of the manuscript. E.R. contributed to the clinical data acquisition and to the critical edition of the manuscript. P.D. co-designed the study concept, performed expert supervision, and clinical examination, contributed to MRI acquisition, and to the critical edition of the manuscript.

Competing interests

The authors declare that there are no financial disclosures or conflicts of interest relevant to this work.

Additional information

Correspondence and requests for materials should be addressed to S. Mareček.

Reprints and permissions information is available at <http://www.nature.com/reprints>

Publisher's note Springer Nature remains neutral with regard to jurisdictional claims in published maps and institutional affiliations.

Open Access This article is licensed under a Creative Commons Attribution 4.0 International License, which permits use, sharing, adaptation, distribution and reproduction in any medium or format, as long as you give appropriate credit to the original author(s) and the source, provide a link to the Creative Commons licence, and indicate if changes were made. The images or other third party material in this article are included in the article's Creative Commons licence, unless indicated otherwise in a credit line to the material. If material is not included in the article's Creative Commons licence and your intended use is not permitted by statutory regulation or exceeds the permitted use, you will need to obtain permission directly from the copyright holder. To view a copy of this licence, visit <http://creativecommons.org/licenses/by/4.0/>.

© The Author(s) 2025